

Sorption Behavior of Radionuclides on Crystalline Synthetic Tunnel Manganese Oxides

Alan Dyer,^{*,†} Martyn Pillinger,[†] Jon Newton,[†] Risto Harjula,[‡]
Teresia Möller,[‡] and Suheel Amin[§]

Chemistry Division, Science Research Institute, Cockcroft Building, University of Salford, Salford M5 4WT, U.K., Laboratory of Radiochemistry, Department of Chemistry, PO Box 55, FI-00014, University of Helsinki, Helsinki, Finland, and British Nuclear Fuels plc, Risley, Warrington, Cheshire WA3 6AS, U.K.

Received July 26, 2000. Revised Manuscript Received September 19, 2000

Cryptomelane-type (potassium) and todorokite-type (magnesium and calcium) manganese oxides were prepared and studied for the removal of radionuclides from aqueous solutions containing inactive metal ions of interest in radionuclide-bearing nuclear waste effluents. Batch distribution coefficients were measured as a function of pH and sodium, potassium, magnesium, and calcium ion concentrations. Trace strontium (⁸⁹Sr) and cesium (¹³⁷Cs) ions were taken up by ion-exchange mechanisms. Selectivity coefficients were estimated as $K_{Cs/K} = 0.6$ and $K_{Sr/K} = 1.0$ for cryptomelane and $K_{Cs/Mg} = 7550$, $K_{Sr/Mg} = 50$, and $K_{Sr/Ca} = 10$ for todorokite. The cryptomelane analogue was particularly effective for the separation of trace silver ions (¹¹⁰Ag) in low-pH solutions. Todorokite analogues were effective for a wider range of radionuclides, including ⁵⁷Co across a wide pH range (1–10) and ¹³⁷Cs in acidic solution. The affinity sequence for magnesium and calcium ion-extracted (acid-treated) todorokites in 0.1 HNO₃ was ¹³⁷Cs > ⁵⁹Fe > ⁵¹Cr ≈ ⁵⁷Co ≈ ²⁴¹Am > ⁵⁴Mn > ⁶³Ni > ⁶⁵Zn > ²³⁶Pu > ⁸⁹Sr.

Introduction

There is an ongoing research effort to develop highly selective ion-exchange materials for the removal of metal radionuclides from aqueous radioactive wastes.^{1,2} This is a challenging task as the radionuclides are usually present at trace concentrations in the presence of large excesses of inactive metal ions. Benefits include large reductions in the volumes of solidified waste and reductions in the radioactive discharges into the environment. Inorganic ion exchangers possess a number of characteristic advantages for these purposes, including superior chemical and thermal stability, good resistance to radiation damage, and good compatibility with final waste forms. Porous inorganic crystals with layered^{3–6} and tunnel^{7–11} structures are particularly promising as they often have high capacities and

selectivities for certain monovalent and divalent cations. New materials are discovered regularly, some of which are analogues of natural minerals, while others have novel structures.

Mixed-valence manganese oxides with tunnel structures are one class of potentially interesting sorbents that can be synthesized in the laboratory.^{12,13} Examples include analogues of the minerals todorokite (channels of 3 × 3 MnO₆ units, tunnel size 6.9 Å, Mg²⁺ in the tunnels)^{14–17} and hollandite (2 × 2, tunnel size 4.6 Å, Ba²⁺ in the tunnels).^{18,19} To date, most of the ion-exchange work on these materials has focused on the characterization of the ion-sieve properties of metal-ion-

* Corresponding author. E-mail: a.dyer@salford.ac.uk.

† University of Salford.

‡ University of Helsinki.

§ British Nuclear Fuel plc.

(1) (a) *Inorganic Ion Exchange Materials*, Clearfield, A., Ed.; CRC Press: Boca Raton, FL, 1982. (b) Clearfield, A. *Ind. Eng. Chem. Res.* **1995**, *34*, 2865–2872.

(2) Lehto, J.; Harjula, R. *Radiochim. Acta* **1999**, *86*, 65–70.

(3) Clearfield, A.; Bortun, A. I.; Bortun, L. N.; Cahill, R. A. *Solvent Extr. Ion Exch.* **1997**, *15*, 285–304.

(4) Bortun, L. N.; Bortun, A. I.; Clearfield, A. In *Ion Exchange Developments and Applications*, Greig, J. A., Ed.; Royal Society of Chemistry: Cambridge, U.K., 1996; pp 313–320.

(5) (a) Kodama, T.; Komarneni, S. *J. Mater. Chem.* **1999**, *9*, 533–539. (b) Kodama, T.; Komarneni, S. *J. Mater. Chem.* **1999**, *9*, 2475–2480.

(6) Lehto, J.; Harjula, R.; Girard, A.-M. *J. Chem. Soc., Dalton Trans.* **1989**, 101.

(7) Poojary, D. M.; Bortun, A. I.; Bortun, L. N.; Clearfield, A. *Inorg. Chem.* **1996**, *35*, 6131.

(8) Bortun, A. I.; Bortun, L. N.; Clearfield, A. *Solvent Extr. Ion Exch.* **1996**, *14*, 341.

(9) Behrens, E. A.; Sylvester, P.; Clearfield, A. *Environ. Sci. Technol.* **1998**, *32*, 101–107.

(10) Dyer, A.; Pillinger, M.; Amin, S. *J. Mater. Chem.* **1999**, *9*, 2481–2487.

(11) Dyer, A.; Pillinger, M. In *Advances in Ion Exchange for Industry and Research*; Williams, P. A., Dyer, A., Eds.; Royal Society of Chemistry: Cambridge, U.K., 1999; pp 261–269.

(12) Brock, S. L.; Duan, N.; Tian, Z. R.; Giraldo, O.; Zhou, H.; Suib, S. L. *Chem. Mater.* **1998**, *10*, 2619–2628.

(13) Feng, Q.; Kanoh, H.; Ooi, K. *J. Mater. Chem.* **1999**, *9*, 319–333.

(14) (a) Golden, D. C.; Chen, C. C.; Dixon, J. B. *Science* **1986**, *231*, 717–719. (b) Golden, D. C.; Chen, C. C.; Dixon, J. B. *Clays Clay Miner.* **1987**, *35*, 271–280.

(15) (a) Shen, Y. F.; Zerger, R. P.; DeGuzman, R. N.; Suib, S. L.; McCurdy, L.; Potter, D. I.; O'Young, C. L. *Science* **1993**, *260*, 511–515. (b) Shen, Y. F.; Suib, S. L.; O'Young, C. L. *J. Am. Chem. Soc.* **1994**, *116*, 11020–11029.

(16) Tian, Z. R.; Yin, Y. G.; Suib, S. L. *Chem. Mater.* **1997**, *9*, 1126–1133.

(17) Feng, Q.; Kanoh, H.; Miyai, Y.; Ooi, K. *Chem. Mater.* **1995**, *7*, 1722–1727.

(18) DeGuzman, R. N.; Shen, Y. F.; Neth, E. J.; Suib, S. L.; O'Young, C. L.; Levine, S.; Newsam, J. M. *Chem. Mater.* **1994**, *6*, 815–821.

(19) Feng, Q.; Kanoh, H.; Miyai, Y.; Ooi, K. *Chem. Mater.* **1995**, *7*, 148.

extracted derivatives by pH titration and distribution coefficient measurement studies.^{13,17,19} This article presents a detailed examination of as-synthesized tunnel manganese oxides for the separation of fission product (¹³⁷Cs, ⁸⁹Sr), activated corrosion product (⁵⁷Co, ⁵¹Cr, ⁵⁴Mn, ⁵⁹Fe, ⁶³Ni, ⁶⁵Zn, ¹¹⁰Ag), and actinide (²³⁶Pu, ²⁴¹Am) radionuclides from aqueous solutions containing competing ions of interest in radionuclide-bearing waste effluents.

Experimental Section

Chemicals used were of reagent-grade quality and were obtained from commercial sources without further purification. Radioisotopes were supplied by Amersham International, Amersham, U.K.

Physical Analyses. Powder X-ray diffraction (XRD) patterns were collected on a Siemens D5000 diffractometer with Cu K α radiation. Water contents in samples preequilibrated over saturated NaCl for 1 week were determined by thermogravimetry (TGA) using a Mettler TA3000 system at a heating rate of 5 K min⁻¹ under a nitrogen atmosphere.

Chemical Analyses. Elemental chemical analyses for sodium, potassium, magnesium, calcium, and manganese were performed by atomic absorption spectroscopy (AAS). About 50 mg of sample was dissolved with 20 mL of double-distilled water (DDW), 1 mL of concentrated nitric acid, and 2 mL of 30% hydrogen peroxide. The colorless solution was boiled for 2–5 min to remove excess peroxide, and the solution was diluted with DDW to 100 mL to make a stock solution.

Average manganese oxidation states were determined using the standard oxalic acid–permanganate back-titration procedure. About 0.2 g of each sample was weighed out and transferred into a 250 mL Erlenmeyer flask containing a 50 mL solution of 10% H₂SO₄ mixed with 0.5 g of Na₂C₂O₄. With mild heating (<100 °C), the samples dissolved completely. KMnO₄ solution (0.02 M, standardized by Na₂C₂O₄ according to the standard method) was then used to back-titrate the excess Na₂C₂O₄.

Preparation of Birnessite-Type Layered Manganese Oxides. Two literature methods were used to prepare Na⁺-birnessite layered manganese oxides. In the first [BIR-1(Na)],¹⁵ a Mn(OH)₂ sol was prepared by addition of 5.0 M NaOH (100 mL) to 0.5 M MnCl₂·4H₂O (80 mL) at room temperature with vigorous stirring. It was then added dropwise to 0.1 M Mg-(MnO₄)₂·6H₂O (70 mL, MnO₄⁻/Mn²⁺ = 0.35) at room temperature with vigorous stirring. The resulting suspension (pH 13.7) was aged at room temperature for 7 days, filtered out, and washed with double-distilled water (DDW) until no chloride was detected.

In the second method [BIR-2(Na)]¹⁴ and 0.5 M MnCl₂ (200 mL) were placed in a plastic beaker. Oxygen was bubbled through a glass frit at a rate of at least 2 L/min. The solution was then treated with a cold solution of 55 g of NaOH in 250 mL of DDW. After 5 h the oxygenation was stopped and the precipitate filtered out and washed with DDW until no chloride was detected.

M²⁺-buserite layered manganese oxides were prepared by ion-exchanging BIR-1(Na) or BIR-2(Na) in 1 M MgCl₂ or Ca-(NO₃)₂ (1 L) while stirring overnight at room temperature. The exchanged products [BUS-1(Mg) and BUS-2(Mg/Ca)] were filtered and washed three times with DDW. Analytical data are given in Table 1.

Preparation of Todorokite-Type Tunnel Manganese Oxides.^{14,15} Washed buserite suspensions were autoclaved at 170 °C for 48 h [BUS-1(Mg)] or 160 °C for 8 h [BUS-2(Mg/Ca)] in Teflon-lined stainless steel vessels to form the corresponding todorokite-type tunnel manganese oxides [TOD-1(Mg) and TOD-2(Mg/Ca)]. The products were isolated by filtration, washed three times with DDW, and air-dried at ambient temperature. Powder XRD and TGA of TOD-1(Mg) were in agreement with ref 15. Observed: Mg, 8.0%; H₂O,

Table 1. Compositional Data for Birnessite-Type Layered Manganese Oxide [BIR-2(Na)], Buserite-Type Layered Manganese Oxides [BUS-2(M)], Todorokite-Type Tunnel Manganese Oxides [TOD-2(M)], and Corresponding Acid-Treated Materials [BUS-2(HM) and TOD-2(HM)]

	Mn (%)	M (%)	M/Mn	H ₂ O (%)	Z _{Mn} ^a
BIR-2(Na)	50.92	7.33	0.344	12.7	
BUS-2(Mg)	45.88	3.11	0.153		3.54
TOD-2(Mg)	51.60	3.44	0.151	15.9	3.81
BUS-2(HMg)	56.27	0.00	0.000		3.98
TOD-2(HMg)	53.16	1.85	0.079	16.9	3.99
BUS-2(Ca)	49.17	4.93	0.137		3.62
TOD-2(Ca)	50.19	4.98	0.136	14.4	3.87
BUS-2(HCa)	54.35	0.02	0.001		4.01
TOD-2(HCa)	54.48	1.12	0.028	15.8	4.23

^a Z_{Mn} = average manganese oxidation state.

12.0% (TGA to 500 °C). Compositional data for TOD-2 materials are given in Table 1.

Metal-ion-extracted manganese oxides were obtained by treating washed and dried BUS-2(Mg/Ca) or TOD-2(Mg/Ca) three times with 1 M HNO₃ (V/m = 50 mL g⁻¹, 1 day for each treatment). The washed and dried products are referred to as BUS-2(HMg/HCa) and TOD-2(HMg/HCa). Compositional data are given in Table 1.

Cryptomelane was prepared using the method described by DeGuzman et al.¹⁸ A solution of KMnO₄ (5.89 g, 37.3 mmol) in DDW (100 mL) was added to a solution of MnSO₄·H₂O (8.8 g, 52.1 mmol) in DDW (30 mL) and concentrated HNO₃ (3 mL). The mixture was autoclaved at 100 °C for 24 h, and the product was filtered out, washed, and dried in air at 120 °C. Powder XRD and TGA were in agreement with ref 18. Observed: K, 8.0%; H₂O, 5.9% (TGA to 500 °C).

Sorption Experiments. Between 25 and 50 mg of exchanger was equilibrated at ambient temperature with solutions spiked with radioactive tracer ions. The reactions were carried out for 1–2 days in 15 mL of polyethylene centrifuge tubes (Elkay) or 20 mL of polyethylene vials (Zinsser) by end over end tumbling. In the “carrier-free” experiments, the concentration of cesium was in the range 2.0 × 10⁻⁸–3.7 × 10⁻⁷ M, the concentration of strontium was in the range 1.5 × 10⁻⁶–3.1 × 10⁻⁶ M, and the concentration of cobalt was in the range 3.6 × 10⁻¹¹–7.3 × 10⁻¹¹ M. ⁵⁷Co tracer, which has a high specific activity, was used to avoid precipitation of cobalt hydroxide in alkaline solutions. The solutions were separated from the solids by centrifugation (15 min at 4000g or 30 000g) followed by filtration through a 0.22 μm poly(vinyl difluoride) membrane (no filtration in the case of ²³⁶Pu). Tracer activities in solution were measured using either a NaI crystal and a single-channel analyzer (⁵¹Cr, ⁵⁴Mn, ⁵⁷Co, ⁵⁹Fe, ⁶³Ni, and ⁶⁵Zn) or a Canberra-Packard 1900 CA tri-Carb liquid scintillation counter (⁵⁷Co, ¹³⁷Cs, and ⁸⁹Sr). Blank determinations were also carried out in order to make corrections for adsorption on contact vials and filters and to check for possible precipitation of radionuclides. Filtrates from all ion-exchange experiments were measured using an Orion model 720A pH meter fitted with an Accumet semi micro calomel electrode.

The distribution coefficient (K_d) was calculated as follows, where A_i and A are the tracer activities before and after treatment, respectively, V is the solution volume (mL), and m is the mass (g) of the manganese oxide:

$$K_d = \frac{(A_i - A) V}{A m} = \frac{\text{concentration of ion in exchanger}}{\text{concentration of ion in solution}} \quad (1)$$

The K_d calculations were based on the hydrated weight of the exchanger. In the determination of K_d as a function of pH, the pH was adjusted by adding concentrated HNO₃ to the solution/exchanger mixture.

Theory

A binary ion exchange reaction between ion A (charge z_A) and ion B (charge z_B) may be written in terms of eq

2,



where overbars refer to the ions in the ion exchanger. The selectivity coefficient is then given by eq 3,

$$K_{A/B} = \frac{\overline{C}_A^{z_B} C_B^{z_A}}{C_B^{z_A} \overline{C}_A^{z_B}} \quad (3)$$

where the \overline{C} values are the concentrations of the ions in the exchanger and C values those in the solution. From eq 1 ($K_d = \overline{C}_A/C_A$) and eq 3 one obtains eq 4.

$$K_d = K_{A/B}^{1/z_B} \left(\frac{\overline{C}_B}{C_B} \right)^{z_A/z_B} \quad (4)$$

Under the special condition that A is present in solution and in exchanger at much lower concentration than B ($\overline{C}_A \ll \overline{C}_B$, $C_A \ll C_B$, e.g., when A is trace cesium ion and B is a macro-ion such as sodium), $K_{A/B}$ and \overline{C}_B are practically constant ($\overline{C}_B \approx Q$, the ion-exchange capacity) and one obtains eq 5 which indicates that a plot of $\log K_d$ against $\log C_B$ should give a straight line with slope $-z_A/z_B$.

$$\log K_d = \frac{1}{z_B} \log(K_{A/B} Q^{z_A}) - \frac{z_A}{z_B} \log C_B \quad (5)$$

Results and Discussion

Preparation of Materials. Literature methods were employed for the synthesis of 2×2 and 3×3 tunnel manganese oxides.^{14,15} The precursor for the synthesis of todorokite-type materials was Na^+ -birnessite, a layered manganese oxide which has a basal spacing of about 10 Å in the wetted state (buserite, double-crystal water sheet) and 7 Å in the dry state (single-crystal water sheet). Buserite samples were prepared by oxidation of $\text{Mn}(\text{OH})_2$ in NaOH with either $\text{Mg}(\text{MnO}_4)_2$ [BIR-1(Na)]¹⁵ or O_2 [BIR-2(Na)].¹⁴ Todorokite samples, designated as TOD-1(Mg) and TOD-2(Mg/Ca), were then obtained by hydrothermal treatment of Mg^{2+} - or Ca^{2+} -exchanged buserites at 160–170 °C. Sample TOD-1(Mg) provided three major peaks in the powder XRD at 9.50, 4.70, and 3.15 Å, very close to that reported previously.¹⁵ Cryptomelane was formed by autoclaving an acidic solution of KMnO_4 and Mn^{2+} at 100 °C [CRY-1(K)].¹⁸

The compositional formulas of TOD-2(Mg) and TOD-2(Ca) can be written as $\text{Mg}_{0.88}\text{Mn}_{5.84}\text{O}_{12} \cdot 4.9\text{H}_2\text{O}$ and $\text{Ca}_{0.79}\text{Mn}_{5.79}\text{O}_{12} \cdot 5.1\text{H}_2\text{O}$, respectively. Chemical analyses indicated that the formation of these materials from the respective buserite precursors was accompanied by an increase in the mean oxidation number of Mn (Z_{Mn} , Table 1). This may be due to a disproportionation of framework Mn^{3+} to Mn^{4+} and Mn^{2+} and to the ejection of some Mn^{2+} into the solution during the synthesis by means of the hydrolysis reaction 6. However, the Mg/Mn and Ca/Mn mole ratios were almost constant before and after hydrothermal treatment. It seems implausible that the M/Mn ratios were maintained by the concomitant release of the required amounts of Mg^{2+} or Ca^{2+} , again by a hydrolysis reaction similar to (6). Instead, it could be that the interlayer Mn^{2+} formed by disproportionation of Mn^{3+} is oxidized back to Mn^{3+} by O_2 in the system and subsequently refills a vacant layer site.

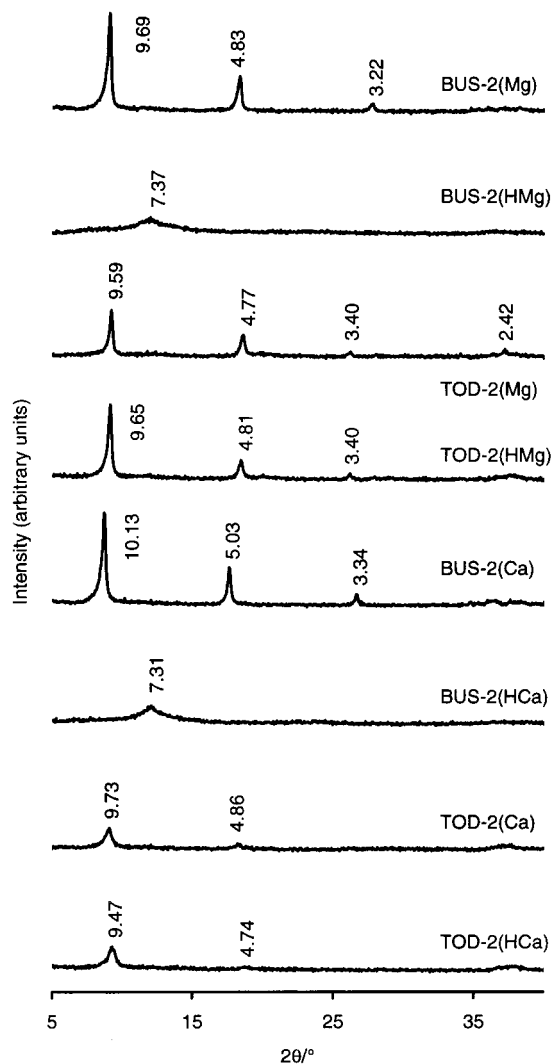
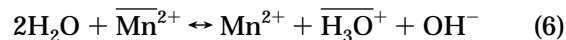


Figure 1. Powder XRD patterns of buserite-type layered manganese oxides [BUS-2(M)], todorokite-type tunnel manganese oxides [TOD-2(M)], and corresponding acid-treated materials [BUS-2(HM) and TOD-2(HM)]. Values adjacent to the diffraction peaks are d -spacings in Å.

tionation of Mn^{3+} is oxidized back to Mn^{3+} by O_2 in the system and subsequently refills a vacant layer site.



Manganese oxide ion sieves have been reported whereby tunnel or interlayer cations in as-synthesized materials are topotactically extracted with acid (Scheme 1).^{13,17,19} The reactions proceed by ion-exchange-type reactions and/or redox-type reactions. Feng et al. reported that 60% of the magnesium ions in a synthetic Mg^{2+} -todorokite were topotactically extracted by treatment with a 1 M HNO_3 solution.¹⁷ Their material was synthesized hydrothermally as in this work but using H_2O_2 instead of O_2 to prepare the precursor Na^+ -birnessite. A similar treatment of sample TOD-2(Mg) resulted in 55% extraction of magnesium ions from the solid. The mean oxidation number of Mn increased to about 4 after the acid treatment, presumably due to complete disproportionation of Mn^{3+} to Mn^{2+} and Mn^{4+} and to the extraction of Mn^{2+} from the tunnel sites (10% of the Mn dissolved). A similar result was obtained with TOD-2(Ca) except that 82% of calcium ions were extracted.

Scheme 1

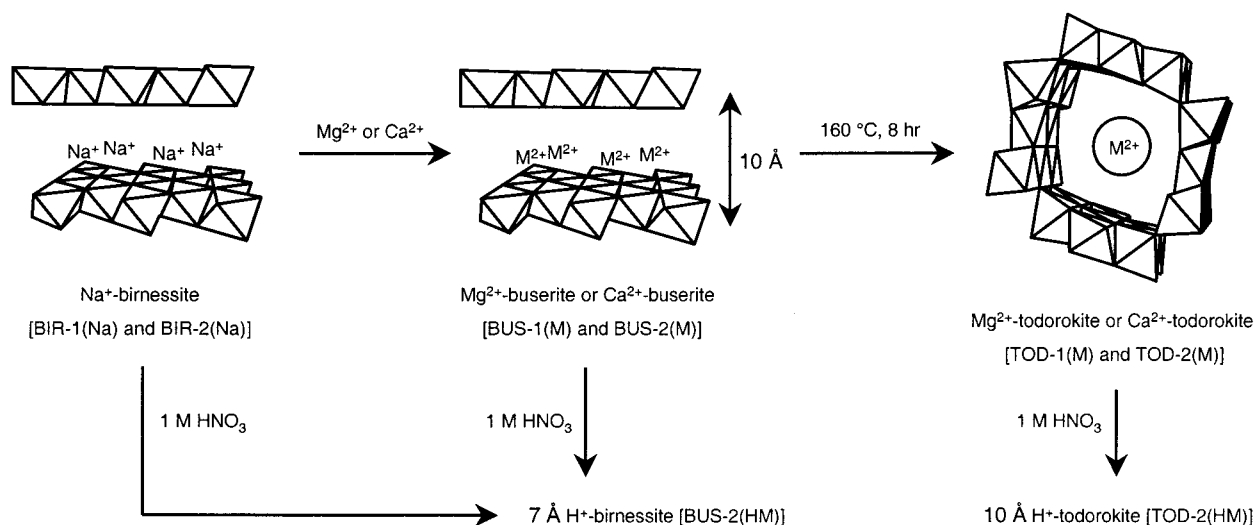


Table 2. Distribution Coefficients of Radionuclides on the Todorokite-Type Manganese Oxide TOD-1(Mg) and the Cryptomelane-Type Manganese Oxide CRY-1(K) (Equilibrium pH in Parentheses, $V/m = 100$ or 200 mL g^{-1})

	deionized H ₂ O		0.1 M NaNO ₃		0.1 M NaNO ₃ , 0.1 M NaOH		0.1 M HNO ₃		4 M HNO ₃	
	CRY-1 (4.07)	TOD-1 (7.20)	CRY-1 (3.43)	TOD-1 (7.00)	CRY-1 (12.95)	TOD-1 (12.96)	CRY-1 (1.08)	TOD-1 (1.20)	CRY-1	TOD-1
¹³⁷ Cs	7420	50 350	185	38	45	5	127	20 700	8	251
⁸⁹ Sr	>10 ⁶	>10 ⁶	149	11 100	>10 ⁶	>10 ⁶	2	1	<0.1	3
⁵⁷ Co	43 300	83 500	32 000	295 600	50	11	24	1 970	<0.1	9
⁵⁴ Mn		45 900		366 500		12 550		290		
⁵⁹ Fe		2820		>10 ⁶		>10 ⁶		24 300		
⁶⁵ Zn	30 850	>10 ⁶	657	716 200	22 800	29 600		9.4	0.5	0.3
¹¹⁰ Ag		593	286 200	1550	1610	5570	71 950	58 400		
²³⁶ Pu	7120	>10 ⁶	447	>10 ⁶	80	14 550	0.3	<0.1	<0.1	0.5

Powder XRD of TOD-2(HMg) and TOD-2(HCa) shows that the extraction reactions proceeded with retention of the todorokite structures (Figure 1). The XRD patterns were similar before and after the acid treatment, except for slight changes in peak positions and relative intensities. Not surprisingly, acid treatment of the precursor M²⁺-buserite materials (9.69 or 10.13 Å basal spacing in the dry state) resulted in complete removal of magnesium or calcium ions and transformation to H⁺-birnessite, which gives a completely different powder XRD pattern in the dry state characteristic of a layered material with a basal spacing of about 7.3 Å (single-crystal water sheet). The fact that not all Mg²⁺ or Ca²⁺ can be extracted from the todorokite materials suggests that hydrothermal treatment of the precursor layered materials results in some Mg²⁺ or Ca²⁺ occupying vacant octahedral sites generated by disproportionation of Mn³⁺.¹⁷ The cations in the tunnel sites can be easily extracted by the acid treatment since they are hydrated ions, but cations in the octahedral sites may not be so easily extracted.

Sorption Studies. Initially, the performance of as-synthesized tunnel manganese oxides for the separation of various radionuclides was assessed by measuring batch distribution coefficients (K_d) in five test solutions (Table 2). In 0.1 M NaNO₃ (pH 7), the todorokite (3 × 3) analogue TOD-1(Mg) performed well for all of the radionuclides studied except ¹³⁷Cs, with K_d s of ⁵⁷Co, ⁵⁴Mn, ⁵⁹Fe, ⁶⁵Zn, and ²³⁶Pu being in excess of 10⁵ mL g^{-1} (99.8% sorption with $V/m = 200$ mL g^{-1}). TOD-1(Mg) was only effective for ¹³⁷Cs in acidic solution, with 99.5%

of cesium ions being removed in 0.1 M HNO₃ and 71.5% in 4 M HNO₃. The same material was also efficient for ⁵⁷Co, ⁵⁹Fe, and ¹¹⁰Ag in 0.1 M HNO₃. Very little radiocobalt was removed from 0.1 M NaNO₃/0.1 M NaOH, presumably due to the formation of Co^{II}(OH)⁺, soluble Co^{II}(OH)₂, and Co^{II}(OH)₃⁻.²⁰ In the case of Fe²⁺, the dominant sorption mechanism probably involves oxidation of Fe²⁺ to Fe³⁺ either on the surface of the manganese oxide or in the tunnels, with concomitant liberation of Mn²⁺. Iron oxide will precipitate except possibly at pH < 2. Even at pH 1, TOD-1(Mg) was very specific for ⁵⁹Fe ($K_d = 24300$ mL g^{-1} , 99.6% sorption).

The cryptomelane (2 × 2) analogue CRY-1(K) was very effective for ⁸⁹Sr in plain distilled water at pH 4, but in 0.1 M NaNO₃ the efficiency was greatly reduced. The same material was very effective for ¹¹⁰Ag at low pH range, even in the presence of sodium ions. Sorption of radiosilver ions reached 99.97% in 0.1 M NaNO₃ (pH 3.4) and 99.86% in 0.1 M HNO₃ ($V/m = 100$ mL g^{-1}). An ion-sieve effect may explain this affinity. K⁺-extracted (acid-treated) cryptomelane-type manganese oxides show specifically high selectivity for the adsorptions of K⁺, Rb⁺, Ba²⁺, and Pb²⁺.^{13,19} Nonhydrated K⁺, Rb⁺, Ba²⁺, and Pb²⁺ have effective ionic radii of 1.52, 1.66, 1.49, and 1.33 Å respectively (6-fold octahedral coordination),²¹ and it has been proposed that the (2 × 2) tunnel has a suitable size for fixing ions having an

(20) Paaajanen, A.; Lehto, J.; Santapakka, T.; Morneau, J. P. *Sep. Sci. Technol.* **1997**, *32*, 813–826.

(21) Shannon, R. D.; Prewitt, C. T. *Acta Crystallogr.* **1969**, *B25*, 925.

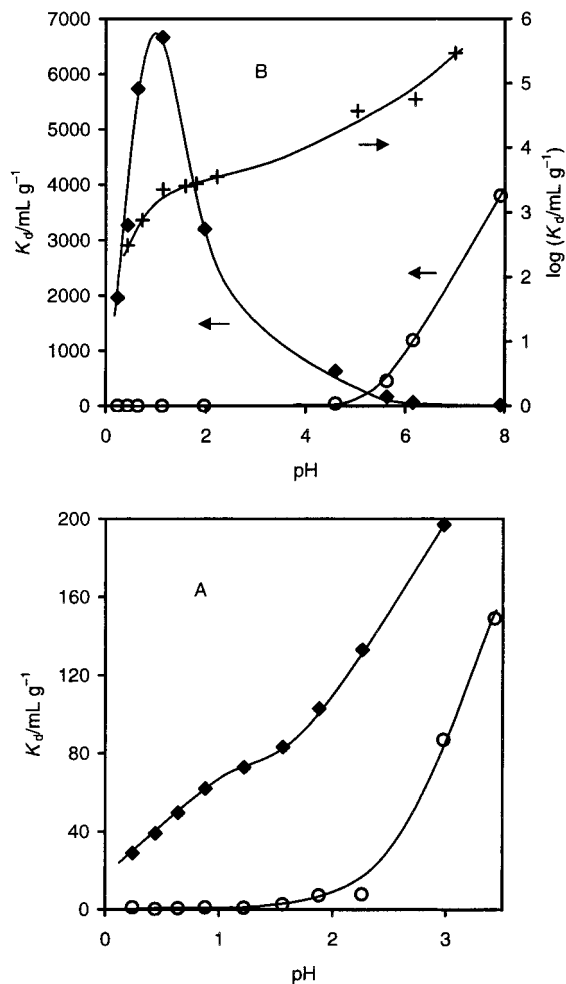


Figure 2. Distribution coefficients of radionuclides on tunnel manganese oxides as a function of pH in 0.1 M NaNO_3 : (A) ^{137}Cs (◆) and ^{89}Sr (○) on cryptomelane [CRY-1(K)]; (B) ^{137}Cs (◆), ^{89}Sr (○), and ^{57}Co (+) on todorokite [TOD-1(Mg)]. $V/m = 100 \text{ mL g}^{-1}$ for ^{137}Cs and ^{89}Sr and 200 mL g^{-1} for ^{57}Co .

effective ionic radius of about 1.4 \AA .^{13,19} The ion Ag^+ , with an effective ionic radius of 1.29 \AA , obviously fits into this group.

The sorption behavior of ^{89}Sr on TOD-1(Mg) as a function of pH in 0.1 M NaNO_3 resembles that of other weak acid inorganic exchangers with layered and tunnel structures, such as sodium titanate,⁶ and titanosilicate analogues of the minerals pharmacosiderite¹⁰ and zorite (Figure 2).¹¹ Below pH 10 the K_d of ^{89}Sr decreased approximately linearly on a logarithmic scale, and at pH 2 practically no strontium was taken up by the exchanger ($K_d < 1 \text{ mL g}^{-1}$). Similar trends were observed for CRY-1(K) in the pH range 1–3.5, although the material performs notably better than TOD-1 in this pH range. For example, at pH 3, CRY-1(K) gave a ^{89}Sr K_d of 90 mL g^{-1} (47% sorption) while TOD-1(Mg) gave a K_d of 2 mL g^{-1} (2% sorption).

The sorption behavior of ^{137}Cs on CRY-1(K) as a function of pH was similar to that observed for ^{89}Sr except that the uptake was slightly higher at any given pH (Figure 2). By contrast, radiocesium uptake on TOD-1(Mg) showed completely different characteristics and was found to increase as the pH was lowered, reaching a maximum of about 6700 mL g^{-1} at pH 1.1. Uptake then decreased sharply as the pH was lowered further. This unusual behavior must be due to a combination of

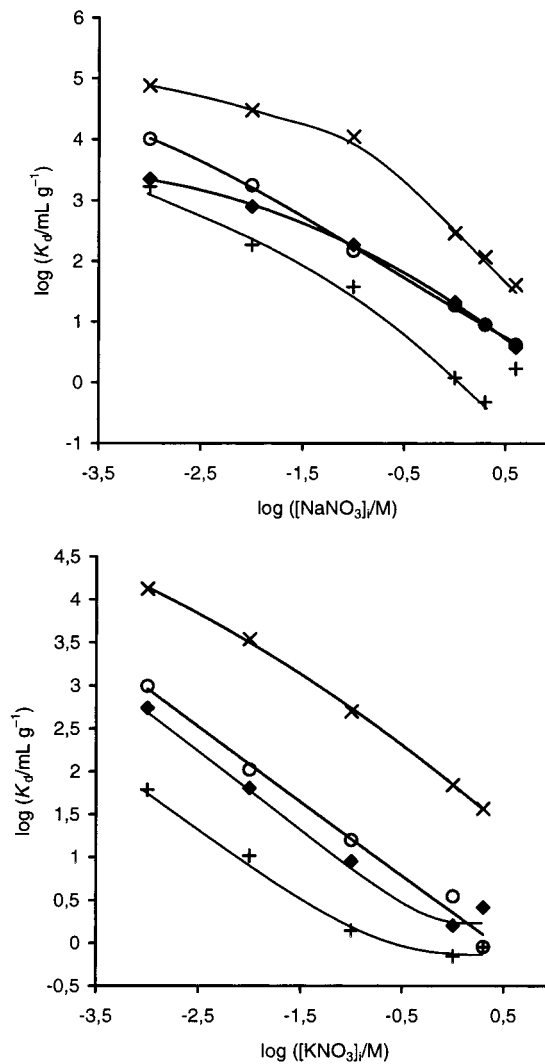


Figure 3. Distribution coefficients of ^{137}Cs (◆) and ^{89}Sr (○) on cryptomelane [CRY-1(K)] and ^{137}Cs (+) and ^{89}Sr (x) on todorokite [TOD-1(Mg)], as a function of sodium ion and potassium ion concentrations ($V/m = 100 \text{ mL g}^{-1}$).

factors, including acid extraction of the magnesium ions from tunnel sites and disproportionation of framework Mn^{3+} to form framework octahedral vacancies. TOD-1(Mg) was highly effective at removing trace cobalt across a wide pH range (1–12, Figure 2). At pH 1, a ^{57}Co K_d of about 1000 mL g^{-1} was achieved. This increased by about 2 orders of magnitude up to pH 7. The high affinity of the todorokite analogue for trace cobalt ions is not surprising given the well-known geochemical association between cobalt and manganese oxides.²²

Distribution coefficients of ^{137}Cs and ^{89}Sr on TOD-1(Mg) and CRY-1(K) were measured as a function of sodium ion and potassium ion concentrations (Figure 3). Uptake of ^{89}Sr on TOD-1(Mg) was very high ($K_d = 10^5\text{--}10^4 \text{ mL g}^{-1}$) for initial sodium nitrate concentrations in the range $0.001\text{--}0.1 \text{ M}$ (equilibrium pH ≈ 7). Toward higher concentrations the ^{89}Sr K_d decreased linearly on a logarithmic scale with a slope of -1.5 (intercept = 2.5). The distribution coefficient of ^{137}Cs on TOD-1(Mg) followed a similar trend but was about 2 orders of

(22) Manceau, A.; Drits, V. A.; Silvester, E.; Bartoli, C.; Lanson, B. *Am. Mineral.* **1997**, *82*, 1150–1175 and references therein.

Table 3. Selectivity Coefficients ($K_{A/B}$) of Trace Cesium and Strontium Exchanges in the Manganese Oxide Todorokite (TOD) and Cryptomelane (CRY) Exchangers

sample	ion pair	Q^a	C^b	linear regression eq	$K_{A/B}$
TOD-1(Mg)	Cs/Mg	6.58	0.001–1.0	$y = 0.49x + 2.34$	7550
TOD-1(Mg)	Sr/Mg	6.58	0.001–1.0	$y = 0.95x + 1.62$	50
TOD-2(Ca)	Sr/Ca	2.49	0.001–0.1	$y = 1.01x + 0.89$	10
CRY-1(K)	Cs/K	2.05	0.001–0.1	$y = 0.89x + 0.05$	0.6
CRY-1(K)	Sr/K	2.05	0.001–0.1	$y = 0.90x + 0.28$	1

^a Theoretical exchange capacities (mequiv g^{-1}) based on the magnesium, calcium, and potassium contents of the hydrated exchangers.

^b Concentration range (M) for linear regression fit to log K_d against log C .

magnitude lower than that of ^{89}Sr at any particular concentration (Figure 3). Sample CRY-1(K), on the other hand, exhibited a similar affinity for both radionuclides and nearly identical distribution coefficients were achieved for initial sodium ion concentrations greater than 0.1 M (equilibrium pH \approx 3.4). A linear relationship was again in evidence (slope = -1.0 , intercept = 1.2).

Similar results were obtained with potassium nitrate (Figure 3). In the potassium ion concentration range 0.001–0.1 M, the ^{137}Cs K_d on CRY-1(K) decreased linearly on a logarithmic scale with a slope of -0.89 , close to the theoretical value of -1 for exchange of a univalent ion for a univalent ion (eq 5). Since CRY-1(K) is in the potassium form, the equilibrium potassium ion concentrations in solution equal the initial ones (except possibly in dilute solution) and trace ion selectivity coefficients, $K_{M/K}$, can be determined from the data presented in Figure 3, using eq 5. A value of 0.6 was obtained (Table 3). In the case of trace strontium exchange, there was also a linear relationship between log K_d and log $[\text{KNO}_3]$, but the slope obtained was -0.90 which differs considerably from the expected value of -2 for exchange of a divalent ion for a univalent ion. This behavior cannot yet be explained. A value of 1.0 was determined for $K_{\text{Sr/K}}$ (Table 3). The low values for the selectivity coefficients confirm that hollandite-type tunnel manganese oxides are highly specific toward K^+ , especially at low-pH range.

Figure 4 shows the distribution coefficient of ^{89}Sr and ^{137}Cs on TOD-1(Mg) and CRY-1(K) as a function of magnesium ion and calcium ion concentrations. Over the magnesium nitrate concentration range studied, the todorokite analogue outperformed the cryptomelane analogue for the removal of both radionuclides. Selectivity coefficients were calculated for TOD-1 as 7750 for $K_{\text{Cs/Mg}}$ and 50 for $K_{\text{Sr/Mg}}$, although these values are probably underestimates as it is assumed that all magnesium ions in the solid are exchangeable. As with TOD-2, it is likely that a certain fraction of the magnesium ions are located in octahedral framework sites and therefore not exchangeable. The pH in the experiments was in the range 7.0–8.0 indicating that only very minor hydrolysis of the magnesium form manganese oxide took place. The slopes for the linear regression fits to log K_d against log $[\text{Mg}(\text{NO}_3)_2]$ were very close to the expected values of -0.5 for pure $\text{Cs}^+/\text{Mg}^{2+}$ exchange and -1.0 for pure $\text{Sr}^{2+}/\text{Mg}^{2+}$ exchange (Table 3). In a separate experiment, TOD-2(Mg) was found to give a ^{89}Sr K_d of 246 $\text{mL } g^{-1}$ in 0.1 M $\text{Mg}(\text{NO}_3)_2$ ($V/m = 100 \text{ mL } g^{-1}$). Using this result with eq 5 gives $K_{\text{Sr/Mg}} = 77$ ($Z_A = 2$, $Z_B = 2$, $Q = 2.8 \text{ mequiv } g^{-1}$), which is similar to that calculated for TOD-1(Mg). If it is assumed that 60% of the Mg^{2+} in this material are exchangeable, one obtains $K_{\text{Sr/Mg}} = 214$.

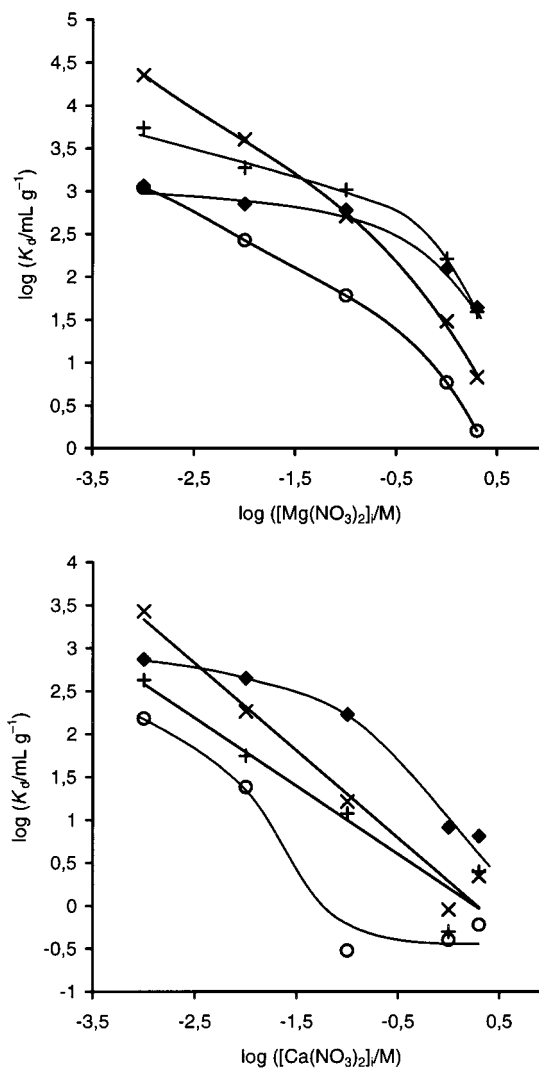


Figure 4. Distribution coefficients of ^{137}Cs (\blacklozenge) and ^{89}Sr (\circ) on cryptomelane [CRY-1(K)] and ^{137}Cs ($+$) and ^{89}Sr (\times) on todorokite [TOD-1(Mg)], as a function of magnesium ion and calcium ion concentrations ($V/m = 100 \text{ mL } g^{-1}$).

As expected, calcium ions had a much greater suppressing effect on trace strontium sorption efficiencies than magnesium ions (Figure 4). TOD-1(Mg) was still better than CRY-1(K), with K_d s being about 10 times higher in the concentration range studied. Calcium ions had a considerably lower influence on radiocesium uptake by CRY-1 compared to TOD-1, with the result that the cryptomelane analogue was more effective than the todorokite analogue for the separation of ^{137}Cs in calcium nitrate solutions. The sorption of ^{89}Sr on TOD-2(Ca) was also studied as a function of calcium nitrate concentration. A linear relationship was again found between log K_d and log $[\text{Ca}(\text{NO}_3)_2]$, giving $K_{\text{Sr/Ca}} \approx 10$ (slope = -1 , pH = 7.3–8.0, $V/m = 100 \text{ mL } g^{-1}$, Table

Table 4. Distribution Coefficients in 0.1 M HNO₃ of the Birnessite-Type Layered Manganese Oxide BIR-2(Na), Buserite-Type Layered Manganese Oxides BUS-2(M), Todorokite-Type Tunnel Manganese Oxides TOD-2(M), and Corresponding Acid-Treated Materials TOD-2(HM) (*V/m* = 200 mL g⁻¹)

	¹³⁷ Cs	⁸⁹ Sr	⁵⁷ Co
BIR-2(Na)	67 250	20.1	5760
BUS-2(Mg)	9 610	11.7	2200
TOD-2(Mg)	1 780	4.6	437
TOD-2(HMg)	5 260	13.1	1190
BUS-2(Ca)	19 400	5.3	2810
TOD-2(Ca)	240 200	29.6	510
TOD-2(HCa)	139 500	21.3	895

3). Bengtsson et al. tested manganese oxides, mixed titanium–manganese oxides, modified carbons, and synthetic and natural zeolites for strontium removal from calcium bearing solutions.²³ K_d s of ⁸⁵Sr were measured in 0.01 M CaCl₂ (pH ≈ 7, *V/m* = 200 mL g⁻¹). The best MnO₂-based sorbents gave K_d s of about 600 mL g⁻¹ while the best synthetic zeolite was Na-zeolite P (K_d = 1400 mL g⁻¹). Natural clinoptilolite samples gave K_d s of between 200 and 400 mL g⁻¹. TOD-2(Ca) gave a K_d of about 1000 mL g⁻¹ in 0.01 M Ca(NO₃)₂ and hence performs on a par with Sr-selective synthetic zeolites. However, it is much less selective than certain octahedral/tetrahedral titanosilicates with tunnel structures such as pharmacosiderite ($K_{Sr/Ca}$ ≈ 370).¹⁰

The todorokite-type products TOD-2(M) and corresponding buserite precursors were screened for the separation of ¹³⁷Cs, ⁸⁹Sr, and ⁵⁷Co from 0.1 M HNO₃ (Table 4). Acid-treated todorokites were also tested. Distribution coefficients of ⁵⁷Co decreased in the order BIR-2(Na) > BIR-2(M) > TOD-2(M/H) > TOD-2(M) (M = Mg or Ca). The uptakes shown by BIR-1 materials were the same as those of BIR-2. Formation of the tunnel manganese oxides was therefore detrimental to trace cobalt sorption efficiencies, although performance was improved by pretreatment with acid. The best material for the removal of ⁸⁹Sr was TOD-2(Ca) (K_d = 30 mL g⁻¹). In contrast to the magnesium form materials, formation of TOD-2(Ca) from BUS-2(Ca) resulted in a significant improvement in performance for ⁸⁹Sr (ca. 6-fold increase in K_d). This was seen even more dramatically for ¹³⁷Cs. Thus, BUS-2(Ca) gave a ¹³⁷Cs K_d of 19 400 mL g⁻¹ in 0.1 M HNO₃, while TOD-2(Ca) gave a K_d of 240 200 mL g⁻¹ under the same conditions (99.92% sorption). This final K_d is more than 2 orders of magnitude higher than that achieved by TOD-2(Mg). The acid-extracted todorokites were tested for the separation of a wider range of radionuclides from 0.1 M HNO₃ (Figure 5). Both materials performed similarly and distribution coefficients decreased in the order ⁵⁹Fe ≫ ⁵¹Cr ≈ ²⁴¹Am > ⁵⁴Mn > ⁶³Ni > ⁶⁵Zn > ²³⁶Pu.

Radiolytic Stability. A sample of TOD-2(Mg) was exposed to 6.1 MGy in the Co-60 source at the University of Salford. Powder XRD indicated no change in the sample crystallinity or composition. As a further test of the materials resistance to radiation damage, the distribution coefficient of ⁸⁹Sr in 0.1 M Mg(NO₃)₂ was measured on the sample before and after irradiation. Again, there was no appreciable change (246 mL g⁻¹ before exposure, 349 mL g⁻¹ after exposure).

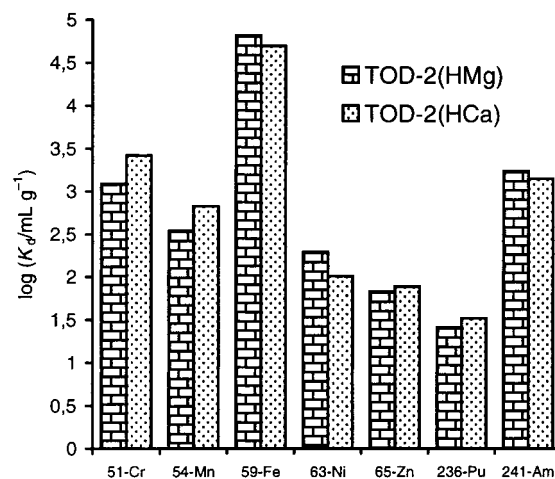


Figure 5. Distribution coefficients of radionuclides in 0.1 M HNO₃ on acid-treated todorokites (*V/m* = 600 mL g⁻¹).

Concluding Remarks

There are only a few industrial-scale applications of inorganic ion exchangers for radioactive waste volume minimization in operation. These mainly involve Cs-selective and Sr-selective materials. The aim of continued research in this area is to find cesium and strontium selective materials which work efficiently in highly acidic and alkaline media and also to find exchangers which are selective for strontium over calcium. In addition, selective exchangers are needed for the activated corrosion products, transuranium elements and anionic fission products (Tc, I). Manganese oxides with tunnel structures constitute a large class of selective ion exchangers and sorbents. In addition to the synthetic cryptomelane- (2 × 2) and todorokite-type (3 × 3) materials studied here, there are several other structure types such as romanachite (2 × 3) and RUB-7 (2 × 4).²⁴ The selectivity of these exchangers toward metal ions depends on their structures. The cryptomelane analogue prepared in this work has a very high affinity for potassium ions but was also effective for the removal of radiosilver ions. The todorokite analogue was effective for a wider range of radionuclides, including cobalt across a wide pH range and cesium in acidic solution. The uptake of trace cesium and strontium on these materials was substantially governed by cation-exchange reactions. Uptake of cobalt is probably more complex, involving a combination of ion exchange and sorption on specific redox sites. Preparation of the todorokite analogue in the calcium form instead of the magnesium form resulted in a very large improvement in performance for cesium in acidic solution and also for strontium over calcium.

Acknowledgment. This study was funded by the European Commission Framework 4 Nuclear Fission Safety Program (Contract FI4W-CT95-0016). The authors also wish to acknowledge all partners in this contract for helpful discussions.

CM001142V

(23) Bengtsson, G. B.; Bortun, A. I.; Strelko, V. V. *J. Radioanal. Nucl. Chem.* **1996**, *204*, 75–82.

(24) Rziha, T.; Gies, H.; Rius, J. *Eur. J. Mineral.* **1996**, *8*, 675–686.